

ARTICLE

Electronic Transport Through $N_{24}B_{24}$ Molecular Junction

Mojtaba Yaghobi*, Mohammad Ali Ramzanpour, Mohammad Reza Nyazian

Ayatollah Amoli Branch, Islamic Azad University, Amol, Iran

(Dated: Received on April 25, 2015; Accepted on March 2, 2016)

We have investigated the electron transport properties of a $N_{24}B_{24}$ molecule coupled to two metallic contacts with a combination of GW approximation and the non-equilibrium Green's-function technique. The calculations indicate that the four and three resonant tunneling peaks are seen for the density of states (DOS) curves in the cases of single and multiple atomic contacts, respectively. The off state and negative differential resistance (NDR) effect are observed in the I - V characteristics of the $N_{24}B_{24}$ molecule. The NDR behavior is also observed in voltages of about ∓ 4.5 , ∓ 4 , ∓ 4.6 , and ∓ 4.3 V for one, four, six, and eight atomic contacts. Also, the I - V characteristics of $N_{24}B_{24}$ are in off state at low voltages that is independent of the contact types. The current curves against the gate voltage depend on contact types and indicate that $N_{24}B_{24}$ molecule behaves as a semiconductor.

Key words: Boron, Nitride, Cage, Electronic transport, Non-equilibrium Green's function**I. INTRODUCTION**

Similar to carbon materials, boron and nitrogen form an interesting family of binary boron nitride (BN) compounds but mechanical, thermal, optical, and catalytic properties of those are different from carbon materials [1–6].

Boron nitride molecules and nanotubes show various electronic, optical and magnetic properties such as Coulomb blockade, photoluminescence and supermagnetism [7]. These properties are important in a large number of possible applications, such as electronic devices, high heat-resistance semiconductors, nanocables, insulator lubricants, and gas storage materials [7–11].

The physical and chemical properties of nano materials depend on their geometries [12–15]. The experimental and theoretical studies indicate that the BN nanotubes and fullerenes are intrinsic semiconductors [16, 17]. Boron-nitride clusters have been made by vacuum arc melting, dissolved in pyridine, and detected using time-of-flight mass spectroscopy, which shows that the $N_{24}B_{24}$ cluster is made in abundance [18]. Computationally, Strout found that boron nitrides (BN) $_n$ have favor cage structures for $n > 10$ [19, 20]. More recently, Strout reported that the boron nitrides ($N_{13}B_{13}$, $N_{14}B_{14}$, and $N_{16}B_{16}$) with squares and hexagons are more stable than the corresponding fullerene-like structures containing pentagons and hexagons [21]. This finding agrees with the results for the $N_{24}B_{24}$ and $N_{30}B_{30}$ cages [22–24]. Pokropivny *et al.* and Wu *et al.*

reported a $N_{24}B_{24}$ structure with twelve squares, eight hexagons and six octagons in O symmetry to be the most stable isomer of any other near spherical molecules [25, 26].

The study of electron transport through single molecules has attracted considerable attention both experimentally and theoretically [27–33]. Electronic transport through single molecules strongly depends on the role of metal/molecule interaction, the energies of the molecular orbitals, in particular, the highest occupied molecular orbital (HOMO) and the lowest unoccupied molecular orbital (LUMO) and the geometry of the contact between the tip and the molecule. Wu *et al.* showed that the coupling between the molecule and the two electrodes and the energy gap between the highest occupied molecular orbital and the lowest unoccupied molecular orbital of the molecule dominate the transport properties [34]. Using a tight-binding model, Paulsson *et al.* indicated that the strength of the metal/molecule interaction and the geometry of the contact between the tip and the molecule play an important role in the drastic increase in the conductance [35]. The study of negative differential resistance (NDR) effect in molecular electronics is a very useful property due to its utility in molecular electronic devices such as molecular switch, logic cell and memory [36, 37]. In this work, we investigate electron transport in single molecule transistors made with the $N_{24}B_{24}$ molecule by considering the effects of contact types and the gate and bias voltages.

II. MODEL AND COMPUTATIONAL METHOD

Figure 1(a) shows a schematic representation of molecular device sandwiched between two semi-infinite

*Author to whom correspondence should be addressed. E-mail: m.yaghoubi@iauamol.ac.ir, Tel.: +98-1212517061 FAX: +98-1212553010

electrodes. The general form of the Hamiltonian of the system is shown as:

$$\hat{H} = \hat{H}_L + \hat{H}_R + \hat{H}_C + \hat{H}_T \quad (1)$$

where \hat{H}_L and \hat{H}_R are the Hamiltonians of the left (L) and right (R) electrodes, \hat{H}_C describes the channel Hamiltonian and \hat{H}_T defines the coupling matrix between the surface atomic orbitals of the leads and the channel. Hamiltonian of electrodes and coupling matrix can be written as:

$$\hat{H}_\alpha = \sum_{(i_\alpha, j_\alpha), \sigma} (\varepsilon_\alpha \delta_{i_\alpha, j_\alpha} - t'_{i_\alpha, j_\alpha}) c_{i_\alpha, \sigma}^+ c_{j_\alpha, \sigma} \quad (\alpha = L, R) \quad (2)$$

$$\hat{H}_T = \sum_{\alpha=\{L, R\}} \sum_{(i_\alpha, j_\alpha), \sigma} (-t_{i_\alpha, j_\alpha}) (c_{i_\alpha, \sigma}^+ d_{j_\alpha, \sigma} + h.c.) \quad (3)$$

here, $t_{i_\alpha, j_\alpha} = t_\alpha$ and $t'_{i_\alpha, j_\alpha} = t'_\alpha$ are the hopping integrals, d_i^+ or c_i^+ (d_i or c_i) is the creation (annihilation) operator for a conduction electron at site i with spin σ ($\sigma = \uparrow, \downarrow$) and ε_α is the on-site energy of the electrodes and will be set to zero. Hamiltonian of central part can be extended as [38, 39]:

$$\hat{H}_C = \sum_i \varepsilon_i d_i^+ d_i + \hat{H}_c^0 + H_c^1 \quad (4)$$

$$H_c^0 = \sum_{\langle i, j \rangle} \sum_\sigma [-t_0 + \alpha' y_{i, j}] (d_{i, \sigma}^+ d_{j, \sigma} + HC) + \frac{1}{2} K (y_{i, j})^2 \quad (5)$$

$$H_c^1 = U_0 \sum_i d_{i, \uparrow}^+ d_{i, \uparrow} d_{i, \downarrow}^+ d_{i, \downarrow} + V_0 \sum_{\langle i, j \rangle} \left(\sum_\sigma d_{i, \sigma}^+ d_{i, \sigma} \right) \left(\sum_{\sigma'} d_{j, \sigma'}^+ d_{j, \sigma'} \right) \quad (6)$$

In above equations, t_0 is the hopping matrix element between nearest-neighboring sites i and j with spin σ ($\sigma = \uparrow, \downarrow$) or σ' , α' presents the electron-phonon coupling constants for the B–N bonds, $y_{i, j}$ is the change of the bond length between the sites i and j , K , and $\langle i, j \rangle$ are the spring constants and the sum over nearest-neighbor pairs for the B–N bonds, respectively, U_0 is the on-site Coulomb repulsion strength and V_0 is the Coulomb strength. Finally, ε_i is the on-site energy where it is equal to gate voltage. The extended method has been described in detail in Refs.[38, 39].

The current-voltage (I - V) characteristic and integral coefficients are calculated, respectively, as follows [40]:

$$I = \frac{ie}{2h} \int_{-\infty}^{\infty} Tr [(f_L \Gamma^L - f_R \Gamma^R) (G^r - G^a) + (\Gamma^L - \Gamma^R) G^<] d\varepsilon \quad (7)$$

$$\text{Coefficients} = Tr [(f_L \Gamma^L - f_R \Gamma^R) (G^r - G^a) + (\Gamma^L - \Gamma^R) G^<] \quad (8)$$

here coupling functions $\Gamma_{L, R}$ are the imaginary parts of the left and right self-energies. The lesser Green's function $G^<$ can be obtained from the Dyson equation and expressed in the general form as [41]:

$$G^<(\varepsilon, V_b, V_g) = G^r(\varepsilon, V_b, V_g) \Sigma^<(\varepsilon, V_b) G^a(\varepsilon, V_b, V_g) \quad (9)$$

The retarded and advanced Green's functions ($G^{r/a}$) of the system can be extended as [41]:

$$G^{r/a}(\varepsilon, V_b, V_g) = \left[\left(\varepsilon - \frac{V_b}{2} \pm i\eta \right) \hat{I} - \hat{H}_c^0(\varepsilon, V_g) - \Sigma_L(\varepsilon, V_b) - \Sigma_R(\varepsilon, V_b) - \Sigma(\varepsilon) \right]^{-1} \quad (10)$$

The lesser self-energy ($\Sigma_{\text{tot}}^<(\varepsilon)$) can be written as follows:

$$\Sigma_{\text{tot}}^< = \Sigma_L^< + \Sigma_R^< + \Sigma^< \quad (11)$$

$$\Sigma_{L/R}^<(\varepsilon, V_b) = -f(\varepsilon - \mu_{L/R}) [\Sigma_{L/R}(\varepsilon, V_b) - \Sigma_{L/R}^+(\varepsilon, V_b)] \quad (12)$$

$$\mu_{L, R} = E_F \mp \frac{1}{2} e V_b \quad (13)$$

where f is the Fermi function, h is the Planck's constant and e is the electron charge [41]. Also, $\mu_{L, R}$ are the electrochemical potentials of the left and right electrodes under the applied bias voltage V_b . E_F is Fermi energy.

Here, Σ_α ($\alpha=L, R$) is the left (L) and right (R) electrodes self-energy matrixes which are given in the Newns-Anderson and Newns's models [41, 42]. These contain the information of the electronic structure of electrodes and their coupling to the molecule. The semi-infinite leads contribute to the scattering region, and this contribution is included through the self-energies in the Green's function of the scattering region.

The full many-body self-energy (Σ) is split into its Hartree and exchange-correlation (xc) parts [43]:

$$\Sigma(\tau, \tau') = \Sigma_h(\tau, \tau') + \Sigma_{\text{xc}}(\tau, \tau') \quad (14)$$

The Hartree term is local in time. The xc- self-energy is nonlocal in time which contains all the complicated many-body effects. We use GW approximation for calculating the xc- self-energy [43]. The GW self-energy can be split into a static exchange (Σ_x) and a dynamic correlation part (Σ_{corr}) as [43]:

$$\Sigma_{\text{xc}}(\tau, \tau') = \Sigma_{\text{GW}}(\tau, \tau') = \Sigma_x \delta(\tau, \tau') + \Sigma_{\text{corr}}(\tau, \tau') \quad (15)$$

The density matrix of the scattering region is calculated from lesser Green's function [44] as:

$$\rho_{ij} = -i \int G_{ij}^<(\varepsilon) d\varepsilon \quad (16)$$

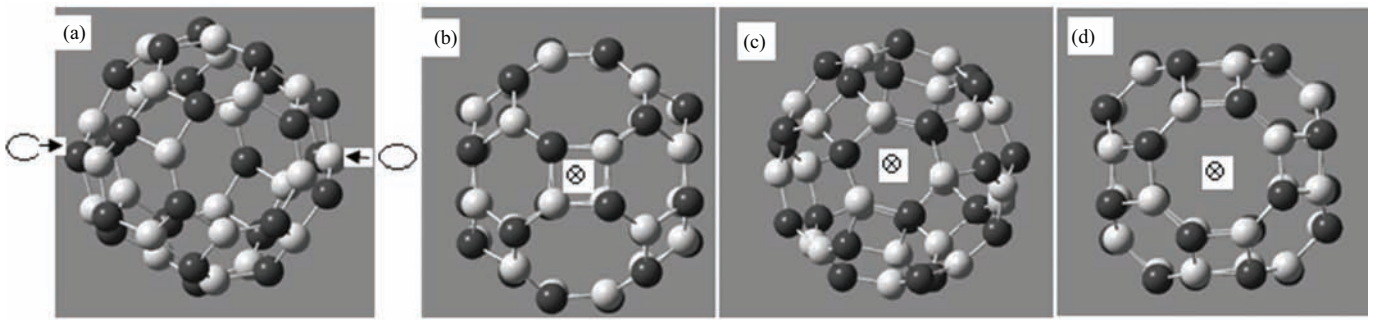


FIG. 1 (a) Geometric configuration of the carbon molecular junction. A $N_{24}B_{24}$ molecule connected to two reservoirs via potential barriers. Schematic view of (b) four, (c) six and (d) eight atomic contacts of $N_{24}B_{24}$ molecule. The central site of contacts has been depicted by a cross inside a circle.

We can also obtain density of state (DOS), defined as:

$$\text{DOS}(\varepsilon) = -\frac{1}{\pi} \text{Im} [\langle i | G^R(\varepsilon) | j \rangle] \quad (17)$$

It should be pointed out that using the charge density, the central part Hamiltonian and the Green's function on every atom in the channel should be iteratively calculated until a convergence of the change of the bond length is reached [38, 39]. Also, the current is determined self-consistently under non-equilibrium condition at every gate voltage.

III. RESULTS AND DISCUSSION

The $N_{24}B_{24}$ molecule can be coupled through an arbitrary number of B and N atoms to two leads that are taken symmetric with respect to the plane passing through the center of mass of the molecule. The $N_{24}B_{24}$ molecule belongs to the O symmetry and B–N bond length is close to that of C–C bond in graphite. Also, it is formed of twelve squares, eight hexagons and six octagons. Therefore, the single or multiple contacts may occur because the direction of the molecule changes the number of contact points when two electrodes are connected to the $N_{24}B_{24}$ molecule. In this work, the coupling through two facing atoms (Fig.1(a)) or squares (Fig.1(b)) or hexagons (Fig.1(c)) or octagons (Fig.1(d)) of molecule to single atom of each electrode will be considered (Fig.1). Here we adopt the following parameters of the model with respect to energy gap and the bond lengths of the $N_{24}B_{24}$ molecule [15] as: $\varepsilon_F=0$ eV, $\varepsilon_0=0$, $t_L=t_R=0.5t_0$, $t_0=2.9$ eV, $t'_L=t'_R=0.8t_0$, $\alpha'=6$ eV/Å, $V=2U=t_0/4$, $T=300$ K, and $K=250.0$ eV/Å².

DOSs as a function of the energy of the incident electron for the $N_{24}B_{24}$ molecule are depicted in Fig.2 with respect to the contact types. The bias voltage is selected $V_b=0$ V. The four and three resonant tunneling peaks are seen in the cases of single and multiple atomic contacts, respectively.

Also, the widths and positions of peaks are varied by changing the contact types. By comparing Fig.2(a)

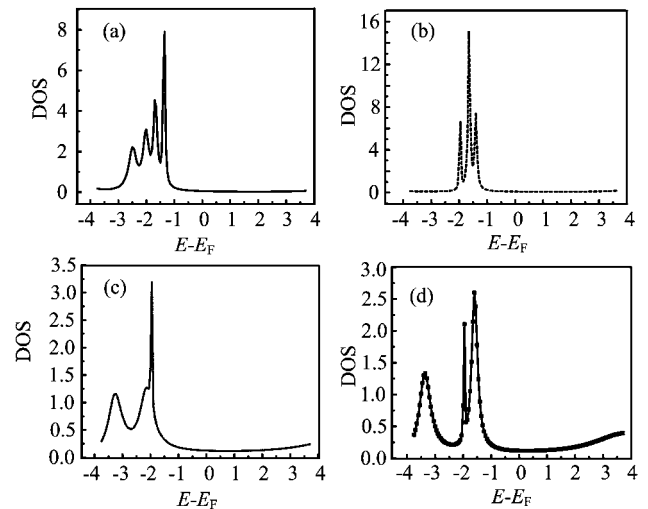


FIG. 2 The DOS coefficients of a $N_{24}B_{24}$ molecule as a function of electron energy for (a) one, (b) four, (c) six, and (d) eight atomic contacts at $V_g=V_b=0$ V.

with Fig.2 (b)–(d), one can easily observe that the number and height of the DOS resonances change with increasing the number of contacts points. On the other hand, the width, height, and the number of the DOS resonances depend on the contact types in the quantum transport that is in accordance with other work [45]. For the region of the bias window $[-3.75, 3.75]$, the significant DOS peaks are in range $E > E_F$ which is independent of contact types.

It is seen that, in most of the energy ranges, the value of DOS is small. The Eq.(9) and Eq.(16) indicate that the DOS coefficient depends on factors of the molecule electronic energy, the contact geometries, and the electrode/molecule coupling strength. Therefore, the Green's function and hence the density of states of the coupled molecule and the DOS spectrum vary with changing the electronic energy of coupled molecule. The large values of the DOS functions are near the molecular levels of $N_{24}B_{24}$ where resonance occurs between the incident electron and the molecular level [46, 47]. There-

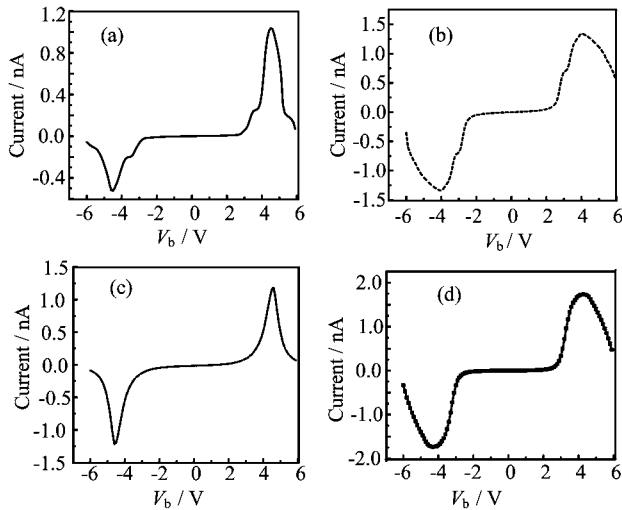


FIG. 3 The electrical current values of $N_{24}B_{24}$ molecule as a function of bias voltage for (a) one, (b) four, (c) six, and (d) eight atomic contacts at $V_g=0$ V.

fore, the DOS spectra strongly depend on the electronic energy and the contact types.

The effect of the contact can be explained as follows. The effect of the contact is described by the coupling and the self-energy matrices. In the case of contact through a single carbon atom of the molecule, only one element of the coupling and the self-energy matrices is non-zero. However, for the transport through opposite four, six, or eight atoms, 16, 36, or 64 elements of the coupling and the self-energy matrices are nonzero, respectively. Therefore, the Greens function and hence the density of states of the coupled molecule and the DOS spectrum vary with changing the number of contacts points.

In Fig.3, the current-voltage (I - V) characteristics of the $N_{24}B_{24}$ have been shown with respect to the contact types. It should be pointed out that the calculated currents are displayed as a function of the applied bias voltage for all systems. The bias voltages are in the range from -6.0 V to 6.0 V in steps of 0.1 V, which is reasonable in practical experimental measurements. Our results represent that I - V characteristics of $N_{24}B_{24}$ are in off state at low voltages. Therefore, a threshold voltage is needed to generate current through the $N_{24}B_{24}$ molecule and then the current increases rapidly with increasing bias voltage. This is due to that the values of DOS near the Fermi level are almost zero and the peaks of DOS are far away from the Fermi level [48]. The threshold voltage is independent of the contact types. Also, the maximum value of current through one atomic contact is smaller than that of multiple atomic contacts. The difference between the I - V characteristics in the single and multiple atomic contacts is due to the change of the coupling matrix and the DOS peaks. The main reason for this is that the hybridization with the electrodes is stronger and there are more paths for the

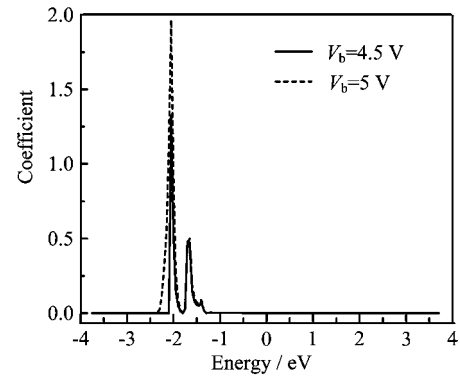


FIG. 4 The integral coefficients of electrical current equation of $N_{24}B_{24}$ molecule as a function of bias voltage for one atomic contact at $V_g=0$ V. The solid and dashed-dotted lines denote the integral coefficients of electrical current equation in $V_b=4.5$ and 5 V, respectively.

electrons that pass from the metal to the molecule with increasing of the number of contacts points between the device electrodes and the molecule.

The I - V characteristics of the $N_{24}B_{24}$ molecule show step-like behavior which is dependent on the contact types. The step-like behavior of the I - V characteristics can be explained by the curve of the DOS coefficients. The experimental and theoretical results of the I - V characteristics for the same systems are qualitatively in agreement with present results with respect to contact types [49].

Overall, the I - V curves of the $N_{24}B_{24}$ molecule have three parts. The first, the value of current is zero, then, increases significantly. Finally, a large NDR is observed in the third part of the I - V curves of the $N_{24}B_{24}$ molecule through both single and multiple atomic contacts. In accordance with our results, the NDR behavior depends on the contact types. The NDR behavior observes about in voltages ∓ 4.5 , ∓ 4 , ∓ 4.6 and ∓ 4.3 V for one, four, six and eight atomic contacts.

We propose the following explanation for the behavior of the NDR. With respect to Eq.(7), it is clear that the current is directly proportional to the area under curve of the integral coefficients. With respect to Eq.(8), Fig.4 indicates the integral coefficients against energy in bias voltages of 4.5 and 5 V for one atomic contacts. Results show that the area under curve decreases in voltage 5 V with respect to that in 4.5 V. Therefore, the total current in voltage 5 V is less than that in 4.5 V and the NDR behavior appears. For additional details see Refs.[50, 51].

Figure 5 shows the current values of the $N_{24}B_{24}$ molecule against the gate voltage with respect to $V_b=0.5$ V. The curves in Fig.5 indicate that the $N_{24}B_{24}$ molecule behaves as a semiconductor for the values of the gate voltages that the total current becomes zero and for the other values those acts as a metal. Such a behavior can be clearly seen in the case that one or

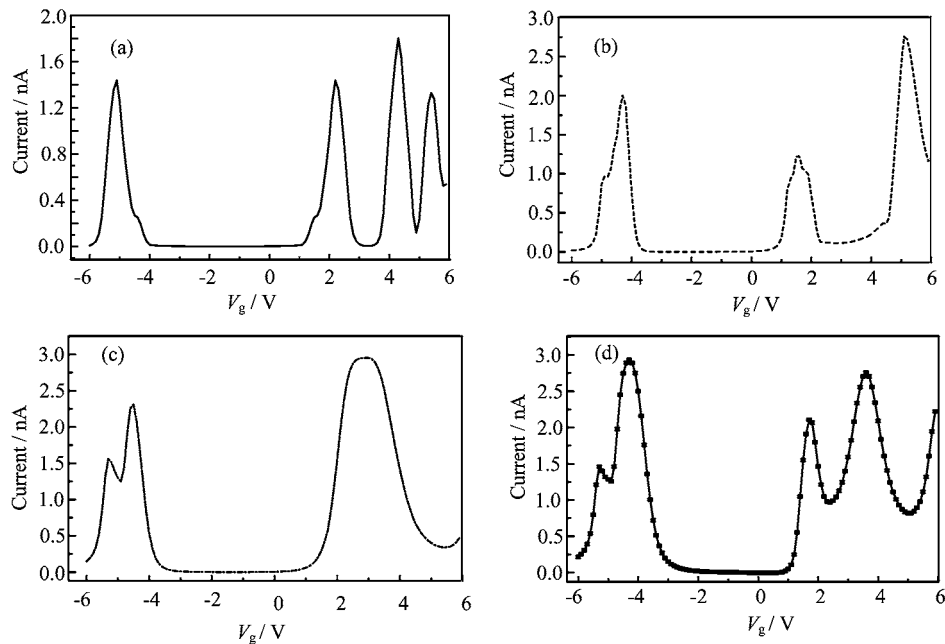


FIG. 5 The electrical current values of the $N_{24}B_{24}$ molecule as a function of gate voltage for (a) one, (b) four, (c) six, and (d) eight atomic contacts at $V_b=0.5$ V.

multiple atoms of the molecule are contacted to the electrodes. The effect of gate voltage is entered by Hamiltonian of central part in the Green's function. Therefore, the Green's function and hence the density of states of the coupled molecule and the current varied with the gate voltage changing.

IV. CONCLUSION

By using the nonequilibrium Green's function technique and the GW approximation, the effects of the contact types and the gate and bias voltages on the electronic transport properties of the $N_{24}B_{24}$ cage sandwiched between two metallic electrodes was investigated. The coupling through two facing atoms or squares or hexagons or octagons of the $N_{24}B_{24}$ molecule to single atom of each electrode considered in calculations. Our results indicate that the effects of types of contacts and the gate and bias voltages are important factors in the electron conduction through a $N_{24}B_{24}$ molecule. Also, NDR behavior is observed in the I - V characteristics of the $N_{24}B_{24}$ molecule. The NDR and step-like behavior of the I - V characteristics of the $N_{24}B_{24}$ molecule are depending on contact types.

[1] Y. Tian, B. Xu, D. Yu, Y. Ma, Y. Wang, Y. Jiang, W. Hu, C. Tang, Y. Gao, K. Luo, Z. Zhao, L. M. Wang, B. Wen, J. He, and Z. Liu, *Nature* **493**, 385 (2013)

- [2] G. Kern, G. Kresse, and J. Hafner, *Phys. Rev. B* **59**, 8551 (1999)
- [3] N. Miyata, K. Moriki, O. Mishima, M. Fujisawa, and T. Hattori, *Phys. Rev. B* **40**, 12028 (1989).
- [4] Y. N. Xu and W. Y. Ching, *Phys. Rev. B* **44**, 7787 (1991).
- [5] N. E. Christensen and L. Gorczyca, *Phys. Rev. B* **50**, 4397 (1994).
- [6] X. Li, J. Zhao, and J. Yang, *J. Sci. Rep.* **3**, 1858 (2013).
- [7] T. Oku, M. Kuno, H. Kitahara, and I. Narita, *Int. J. Inorg. Mater.* **3**, 597 (2001).
- [8] T. Oku, T. Hirano, M. Kuno, T. Kusunose, K. Niihara, and K. Suganuma, *Mater. Sci. Eng. B* **74**, 206 (2000).
- [9] W. Mickelson, S. Aloni, W. Q. Han, J. Cumings, and A. Zettl, *Science* **300**, 467 (2003).
- [10] T. Oku, K. Hiraga, T. Matsuda, T. Hirai, and M. Hirabayashi, *Diamond Relat. Mater.* **12**, 1138 (2003).
- [11] T. Oku, K. Hiraga, T. Matsuda, T. Hirai, and M. Hirabayashi, *Diamond Relat. Mater.* **12**, 1918 (2003).
- [12] S. Iijima, *Nature* **354**, 56 (1991).
- [13] R. Saito, G. Dresselhaus, and M. S. Dresselhaus, *Physical Properties of Carbon Nanotubes*, London: Imperial College Press, (1998).
- [14] M. Fujita, K. Wakabayashi, K. Nakada, and K. Kusakabe, *J. Phys. Soc. Jpn.* **65**, 1920 (1996).
- [15] M. Yaghobi and M. Yaghobi, *Mol. Phys.* **112**, 206 (2014).
- [16] A. Rubio, L. Jennifer, L. Corkill, and M. L. Cohen, *Phys. Rev. B* **49**, 5081 (1994).
- [17] R. Arenal, O. Stephan, M. Kociak, D. Taverna, A. Loiseau, and C. Colliex, *Phys. Rev. Lett.* **95**, 127601 (2005).
- [18] T. Oku, A. Nishiwaki, I. Narita, and M. Gonda, *Chem. Phys. Lett.* **380**, 620 (2003).
- [19] D. L. Strout, *J. Phys. Chem. A* **104**, 3364 (2000).

- [20] D. L. Strout, *J. Phys. Chem. A* **105**, 261 (2001).
- [21] D. L. Strout, *Chem. Phys. Lett.* **383**, 95 (2004).
- [22] H. S. Wu, X. H. Xu, F. Q. Zhang, and H. Jiao, *J. Phys. Chem. A* **107**, 6609 (2003).
- [23] M. L. Sun, Z. Slanina, and S. L. Lee, *Chem. Phys. Lett.* **233**, 279 (1995).
- [24] Z. Slanina, M. L. Sun, and S. L. Lee, *Nano Struct. Mater.* **8**, 623 (1997).
- [25] V. V. Pokropivny, V. V. Skorokhod, G. S. Oleinik, A. V. Kurdyumov, T. S. Bartnitskaya, A. V. Pokropivny, A. G. Sisonyuk, and D. M. Sceichenko, *J. Solid State Chem.* **154**, 154 (2000).
- [26] H. S. Wu and H. Jiao, *Chem. Phys. Lett.* **386**, 369 (2004).
- [27] T. H. Park and M. Galperin, *Phys. Scr. T* **151**, 014038 (2012).
- [28] M. A. Reed, C. Zhou, C. J. Muller, T. P. Burgin, and J. M. Tour, *Science* **278**, 252 (1997).
- [29] R. H. M. Smit, Y. Noat, C. Untiedt, N. D. Lang, M. C. van Hemert, and J. M. van Ruitenbeek, *Nature* **419**, 906 (2002).
- [30] (a) M. yaghobi and F. A. Larijani, *Pramana J. Phys.* **84**, 155 (2015).
(b) S. A. Ketabi, H. Milani Moghaddam, and N. Shah-tahmasebi, *Pramana J. Phys.* **69**, 661 (2007).
- [31] S. Yamacli, *Phys. Scr.* **82**, 045705 (2010).
- [32] B. N. J. Persson and N. G. van Kempen, *Phys. Scr.* **38**, 282 (1988).
- [33] F. Cataldo, G. Strazzulla, and S. Iglesias-Groth, *Mon. Not. R. A. Stron Soc.* **394**, 615 (2009).
- [34] J. Q. Lu, J. Wu, H. Chen, W. Duan, B. L. Gu, and Y. Kawazoe, *Phys. Lett. A* **323**, 154 (2004).
- [35] M. Paulsson and S. Stafström, *J. Phys.: Condens. Matter* **11**, 3555 (1999).
- [36] D. A. Wharam, T. J. Thornton, R. Newbury, M. Pepper, H. Ahmed, J. E. F. Frost, D. G. Hasko, D. C. Peacock, D. A. Ritchie, and G. A. C Jones, *J. Phys. C* **21**, L209 (1988).
- [37] S. Sze, *Physics of Semiconductor Devices*, New York: Wiley, (1981).
- [38] R. H. Xie, *Phys. Lett. A* **258**, 51 (1999).
- [39] R. H. Xie and Q. Rao, *Chem. Phys. Lett.* **313**, 211 (1999).
- [40] Y. Meir and N. S. Wingreen, *Phys. Rev. Lett.* **68**, 2512 (1992).
- [41] D. M. Newns, *Phys. Rev.* **178**, 1123 (1969).
- [42] P. W. Anderson, *Phys. Rev.* **124**, 41 (1961).
- [43] K. S. Thygesen *Ph.D. Dissertation*, CAMP: Department of Physics, Technical University of Denmark, (2005).
- [44] S. Datta, *Electronic Transport in Mesoscopic Systems*, New York: Cambridge University Press, (1995).
- [45] L. Wang, K. Tagami, and M. Tsukada, *Jpn. J. Appl. Phys.* **43**, 2779 (2004).
- [46] (a) J. Taylor, H. Guo, and J. Wang, *Phys. Rev. B* **63**, R121104 (2001).
(b) T. Seideman and H. Guo, *J. Theor. Comput. Chem.* **2**, 439 (2003).
(c) A. Sinha, *Resonance* **6**, 55 (2001).
- [47] L. G. Wang, K. Tagami, and M. Tsukada, *Jpn. J. Appl. Phys.* **43**, 2779 (2004).
- [48] X. F. Li, K. Q. Chen, L. Wang, and Y. Luo, *J. Phys. Chem. C* **114**, 12335 (2010).
- [49] (a) C. Joachim and J. K. Gimzewski, *Eur. Phys. Lett.* **30**, 409 (1995).
(b) D. Porath, Y. Levi, M. Tarabiah, and O. Millo, *Phys. Rev. B* **56**, 9829 (1997).
(c) D. Porath and O. Millo, *J. Appl. Phys.* **81**, 2241 (1997).
- [50] (a) X. F. Li, K. Q. Chen, L. Wang, M. Q. Long, and B. S. Zou, *Appl. Phys. Lett.* **91**, 133511 (2007).
(b) X. F. Li, K. Y. Lian, Q. Qiu, and Y. Luo, *Nanoscale* **7**, 4156 (2015).
- [51] M. Yaghobi and H. R. Vanaie, *Phys. Lett. A* **375**, 1249 (2011).